A Hybrid Super-Resolution Method for Medical Images Using Transfer Learning

Amir Hossein Jalalzadeh[1] and Mehrdad Hashemi Kamangar[2*]
[1] Department of Biomedical Engineering, Faculty of Engineering, Shahed University, Persian Gulf Expressway, Opposite Imam Khomeini Holy Shrine, Tehran, Iran
[2] Department of Electrical and Electronic Engineering, Faculty of Engineering, Shomal University, Haraz Road, Amol, Mazandaran Province, Iran
*e-mail: mh.kamangar@shomal.ac.ir

Abstract. High-quality medical imaging is essential for accurate diagnosis and effective treatment planning. However, limitations such as noise, artifacts, high acquisition costs, and patient safety concerns often restrict the ability to obtain high-resolution (HR) scans. Super-resolution (SR) techniques offer a promising alternative by reconstructing HR images from low-resolution (LR) inputs, thereby enhancing image quality without additional scanning. This capability is particularly important in clinical contexts, where improving image resolution directly impacts diagnostic confidence and therapeutic decision-making. In this work, we propose a hybrid SR framework that integrates transfer learning with a generative adversarial network (RESRGAN) and low-rank total variation (LRTV) regularization. This combination leverages both local neighborhood features and global contextual information to recover fine structural details while preserving overall image fidelity. The approach was evaluated on three brain imaging modalities – magnetic resonance imaging (MRI), computed tomography (CT), and ultrasound – using volumetric datasets acquired at different time intervals. Quantitative experiments show that the proposed method consistently outperforms bicubic interpolation, achieving an average peak signal-to-noise ratio (PSNR) of 40.05 dB and a structural similarity index (SSIM) of 0.9808. Notably, ultrasound images exhibited the most substantial improvement. These findings highlight the potential of the proposed framework as a robust tool for enhancing medical image quality and supporting more reliable clinical decision-making.

Keywords: medical image processing; super-resolution; deep neural network; MRI; CT Scan; ultrasound.

Paper #9342 received 27 Aug 2025; revised manuscript received 2 Oct 2025; accepted for publication 10 Oct 2025; published online 12 Dec 2025. doi: 10.18287/JBPE25.11.040304.

1 Introduction

In recent years, researchers in both image system manufacturing and software development have strived to create digital images with high quality and resolution. Medical images are particularly challenging due to their importance in image reconstruction and generation [1]. As doctors rely on images for patient diagnosis and treatment, the significance of this challenge will only continue to grow [2]. A thorough comprehension of medical image observation and review is essential for informed decision-making and improved treatment of patients. Recent technological advancements have significantly increased the accuracy and quality of medical imaging systems. However, obtaining high-quality images in medical centers remains a persistent challenge due to factors such as noise, artifacts, and the high cost of modern equipment. Improving image quality using super-resolution methods has become a popular research topic among experts in the medical, industrial, and laboratory fields due to the necessity of each level of image processing, such as noise removal, segmentation, registration, object recognition, etc. [3−7]. Most of these techniques have been applied to general digital images. As image quality increases, it is critical to preserve important medical information after translations. It is important to compare and review the current proposed methods, particularly for medical images. The super-resolution will be mainly divided into two categories:

1 − multi image super-resolution (MISR);

2 − single image super-resolution (SISR).

In the initial approach, we acquire multiple images of an object with average qualities using techniques such as image averaging, conversion of images to the frequency domain and amplification of high frequencies, or merging information from several images. As a result, we obtain high resolution, also referred to as super-resolution MISR. For our study, we will employ the SISR method. Due to existing limitations, such as time-consuming medical imaging processes, the risk of high-dose radiation exposure and tissue ionization, as well as high costs, recording multiple patient images is not feasible. This presents a significant challenge for super-resolution of medical images compared to other digital images. Thus, we will utilize the SISR method. Starting with the original image, known as high resolution (HR), we will create a low-resolution (LR) image. The quality and resolution will be improved via various methods, including interpolation and up-sampling, using only the information from the HR image. Notably, previous studies on medical images implementing super-resolution methods utilized single-modality images [8]. In this study, we evaluated three distinct image modalities. Both non-neural network methods [9, 10] and deep neural networks [11] can generate super-resolution images. Artificial neural networks have made this algorithm highly popular in machine learning due to its efficiency. Deep neural networks have shown their capability to solve problems such as classification and regression across multiple domains.

In the past few years, progress has been made in the use of deep networks for super-resolution applications, with promising results. Generative adversarial networks, known as GAN, will be very powerful in this field [12−15]. The GAN architecture was first described in the 2014 paper by Goodfellow et al. [16]. They must compete with an adversary by generating samples directly. In addition, the discriminator network tries to distinguish between samples from the training data and samples generated by the generator [17, 18].

The primary aim of this research is to develop and evaluate a novel approach for enhancing the quality of medical images through super-resolution techniques, leveraging transfer learning and the RESRGAN network [19] combined with the total variation method [20]. This study focuses on three distinct medical imaging modalities − computed tomography (CT) scan, magnetic resonance imaging (MRI), and ultrasound − to improve the resolution of low-quality images while preserving critical medical information. It addresses key challenges in medical imaging, including time constraints, high costs, and radiation exposure risks, thereby contributing to more effective diagnostic and therapeutic outcomes.

1.1 Previous Works

Akbari et al. [21] used the random forest method for super-resolution of abdominal CT scan images. In this work, they first divided CT slice images into non-overlapping patches and used deep learning networks to cluster them during the training phase. To prepare LR images, a Gaussian filter was first applied to the image, and the dimensions of the image were reduced, finally, non-overlapping patches with a size of 5×5 pixels were considered as input to the random forest algorithm to reconstruct HR images. Finally, they validated their work using peak signal-to-noise ratio (PSNR) and structural similarity index measure (SSIM) metrics, and the obtained results show an improvement in the values compared to the bicubic method. The proposed algorithm for PSNR and SSIM showed an improvement of 5.6 dB and 0.11, respectively.

Deeba et al. [22] also introduced a wavelet-based super-resolution method using a convolutional neural network. Instead of a discrete wavelet transform, they utilized a stationary wavelet transform. Then for training, a 3-layer neural network is considered, after the hidden layer, using the sub-pixel convolution technique, this technique directly creates HR images by using an upscaling filter for each feature map of the LR image [23]. Their method was trained and tested using 662 radiology images, and the reported scores for the two PSNR and SSIM metrics are 31.65 and 0.92, respectively.

Gu et al. [24] increased the resolution of CT scans and MR images using an adversarial generative network based on deep learning. In this work, in addition to using the residual whole map attention network (RWMAN) network as a generator of all aspects of the image, they focused more on the significant parts of the image and also benefited from the weighted sum of losses during training. Training and validation of the network have been done using 242 CT images and 110 MR brain images, and the final result of the algorithm, in addition to the common metrics of PSNR and SSIM, has been reviewed and evaluated by the empirical metrics of the average opinions of 5 radiologists as experts. The PSNR metric increased by 3.3 and the SSIM metric increased by 0.005 compared to the bicubic method for CT scan images.

In another work, Chen et al. [25] also implemented a super-resolution algorithm for medical images based on deep learning. Their convolutional neural network is constructed using adaptive weighted recurrent connections, which was named feedback adaptively weighted dense network (FAWDN). The output information from the image is passed to the LR image property page through recursive connections in this method. Also, to obtain more information from the image, the adaptive weight feature has been used to avoid receiving overlapping data by adaptively selecting advanced features that contain important information from the image. The network was trained by using multiple medical datasets that contained MR images of various body organs in this work. The results obtained on average from one dataset for PSNR metric was 31.57 and for SSIM was 0.90.

In another method based on non-deep neural networks, Salvador et al. [26] working on public images were able to present a new method in super-resolution. A set of public digital images was used to implement their algorithm. In this work, by applying Bayes theorem and bimodal trees for clustering, and in the next step, mapping each image patch using local Bayesian, they increased the work speed and improved the PSNR metric of the output images. According to the results, there will be a slight increase in PSNR amount with the increase in clusters. The only work evaluation index used in this work was PSNR, and the changes in the results caused by the increase of clusters were not taken into account.

2 Materials and Methods

2.1 Data

In this work, to make the results comprehensive and positive performance of the model on medical images, we used three different modalities of medical images. Different reconstructed images are obtained using different technologies. There is no overlap between the three databases used in this project and they are completely separate from one another. The first database is the 3D brain MR images of 23 men and women, from (St. Olav's University Hospital, Trondheim, Norway), which was obtained after the informed consent of the patients during the years 2011 to 2016. The images were created using a 3T Magnetom Skyra MRI scanner (Siemens, Erlangen, Germany) with a 20-channel head coil for 12 min. T2 images were utilized in this project. Also, this database contains brain ultrasound images of the same people after skull removal. The obtained 3D ultrasound images were prepared using the Sonowand Invite neuronavigation system (Sonowand AS, Trondheim, Norway). Also, a linear probe in the frequency range of 6 to 12 MHz was used. The Sonowand Invite neuronavigation system utilized a Polaris infra-red camera (manufactured by NDI, Waterloo, Canada) to accurately record the position and orientation of the ultrasound probe. This was achieved through the optical trackers that were securely attached to the probe [27]. Another database deals with 3D brain CT scan images from the Patient Contributed Image Repository (PCIR) [28] open-access database, which includes medical images of different organs and different techniques. The brain CT scan data recorded in 2006 in digital imaging and communications in medicine (DICOM) format was utilized in this work. A sample of the data used can be seen in the Fig. 1.

It should be mentioned that Mango software was used to display images [29] and MATLAB software [30] was used for 3D volume display. Representative 3D samples of the imaging modalities are shown in Fig. 2.

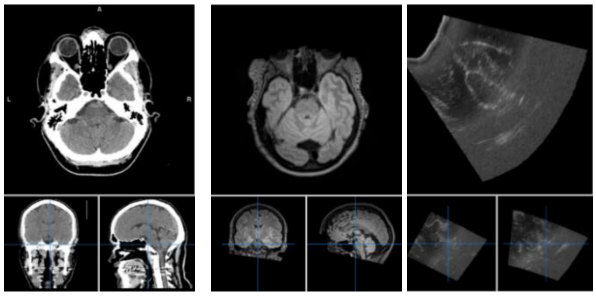

(a) (b) (c)

Fig. 1 Two-dimensional representations of sample data images from three imaging modalities. (a) CT scan sourced from the PCIR database; (b) MRI and (c) ultrasound images obtained from the REtroSpective evaluation of cerebral tumors (RESECT) database [27].

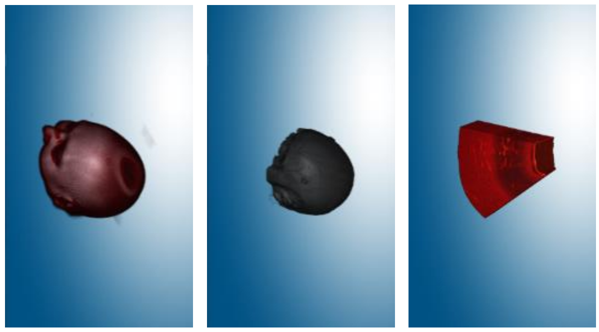

(a) (b) (c)

Fig. 2 Representative samples of volumetric 3D data images, showcasing diverse medical imaging modalities. (a) CT scan with dimensions 64×256×256 voxels, sourced from the PCIR database; (b) MRI and (c) ultrasound images obtained from the RESECT database [27], with MRI dimensions of 192×256×256 voxels and ultrasound dimensions of 348×313×275 voxels.

2.2 Pre-Processing

All high-resolution images will be available to us because the data sets were not recorded specifically for super-resolution processing. To obtain LR images as training data, it is necessary to create LR images that correspond to each of the data using existing processes and use them as input to the proposed algorithm.

The Gaussian function filter shown in Eq. (1) was used to smooth all the images first. We picked 0.5 for the variance of the considered filter.

$$G_{(x,y)} = \frac{1}{2\pi\sigma^2} e^{\frac{x^2+y^2}{2\sigma^2}}. \tag{1}$$

In the next step, we reduced the dimensions of the images by applying Eq. (2) with a factor of 1/2 for all images in all directions. This resulted in an output image with half the dimensions of the input image. Bicubic interpolation was used as the interpolator function for each slice of the image during this translation.

$$\begin{bmatrix} x_0 & y_0 & 1 \end{bmatrix} = \begin{bmatrix} x_i & y_i & 1 \end{bmatrix} \begin{bmatrix} 1 & 0 & 0 \\ 0 & 1 & 0 \\ t_x & t_y & 1 \end{bmatrix}. \qquad (2)$$

In this equation, y_i and x_i represent the dimensions of the input image, y_0 and x_0 represent the dimensions of the output image, also t represents the displacement of each pixel in different directions.

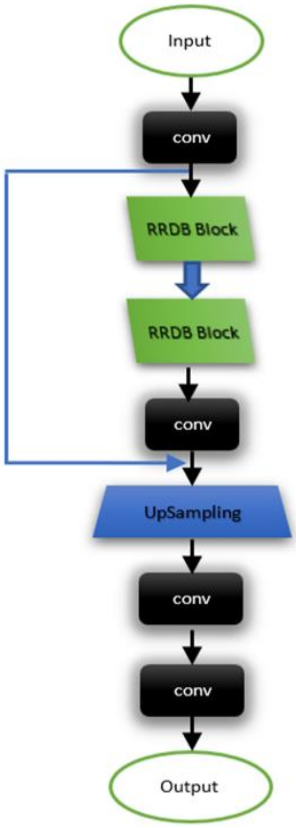

Fig. 3 Schematic representation of the RESRGAN network architecture employed for super-resolution reconstruction in medical imaging. The diagram delineates the sequential layers: black blocks correspond to convolutional operators responsible for feature extraction and transformation; the blue block indicates the upsampling module, which facilitates spatial resolution augmentation through techniques such as pixel shuffling; and green blocks represent residual in residual dense blocks (RRDB), designed to enhance deep feature propagation and mitigate vanishing gradient issues via nested residual connections.

2.3 Proposed Method

The LR image is inputted into the low-rank and total variation (LRTV) method to super-resolution. This method utilizes the neighborhood information of the pixels, as well as the general information and voxel placement of the image to improve the quality of the reconstruction. Neighborhood information is the sole factor that can retain the sharpness of edges in a given image. To optimize this method, alternating direction method of multipliers (ADMM) is employed as the optimizer function. Finally, the pre-trained RESRGAN network receives the image for further processing. Just like other adversarial generator networks, this network has two parts including generator and discriminator. The generator network receives the LR image as an input and the discriminator network tries to minimize the difference between the output image made by the generator network and the original image. The generative network does not just upscale the image, but also returns the details of the image according to the initial information obtained from the previous method. Also, as shown in Fig. 3, this network RRDB to enhance the quality of the final reconstructed image. The *U*-net model is followed by the adversarial network in this architecture, which utilizes spectral normalization to enhance stability while training. Figure 4 presents an overview of the steps taken in this project to create high-resolution medical images.

3 Results

To evaluate this work, image similarity measurement methods are necessary. Because of the absence of a specific standard for these issues, it is essential to utilize the current metrics. In previous articles and other research, SSIM and PSNR Metrics were used to evaluate their methods [31, 32]. It should be noted that other Metrics are also available, such as sum of squared differences (SSD), correlation coefficient (CC), etc. To compare with previous works, we concentrate on two metrics, PSNR and SSIM, in this project. The two LR images super-resolved by the proposed method and the original HR image are examined from the point of view of similarity, and the higher the similarity, the better the result.

The SSIM index is a measure of image structural similarity that measures the similarity of two images by examining the dependence of pixels on their neighbors. Since the neighborhood of pixels in the image also contains important information, it can be concluded that by examining this information, the structure of the objects in the images can be compared [33]. Eq. (3) shows how to calculate this index:

$$SSIM_{(X,Y)} = \frac{(2u_x u_y + C_1)(2\sigma_{xy} + C_2)}{(u_x^2 + u_y^2 + C_1)(\sigma_x^2 + \sigma_y^2 + C_2)}, \qquad (3)$$

where u_x , u_y represent the mean and σ_x , σ_y represent the standard deviation of x and y values. Also, σ_{xy} is the covariance of x, y and the values indicated by the letter C are constant values. The final range of SSIM is between the numbers 0 and 1, where the number 0 indicates no similarity and the number 1 indicates complete similarity between the two images.

The PSNR metric is also a similarity index based on the amount of signal (here pixels of an image) to the amount of noise [34]. Equations (4−5) is the method of calculating this metric:

$$MSE = \frac{1}{mn}\sum_{j=0}^{m-1}\sum_{k=0}^{n-1}[I_{HR}(j,k) - I_{SR}(j,k)]^2, \quad (4)$$

$$PSNR = 20\log\left(\frac{255}{\sqrt{MSE}}\right). \quad (5)$$

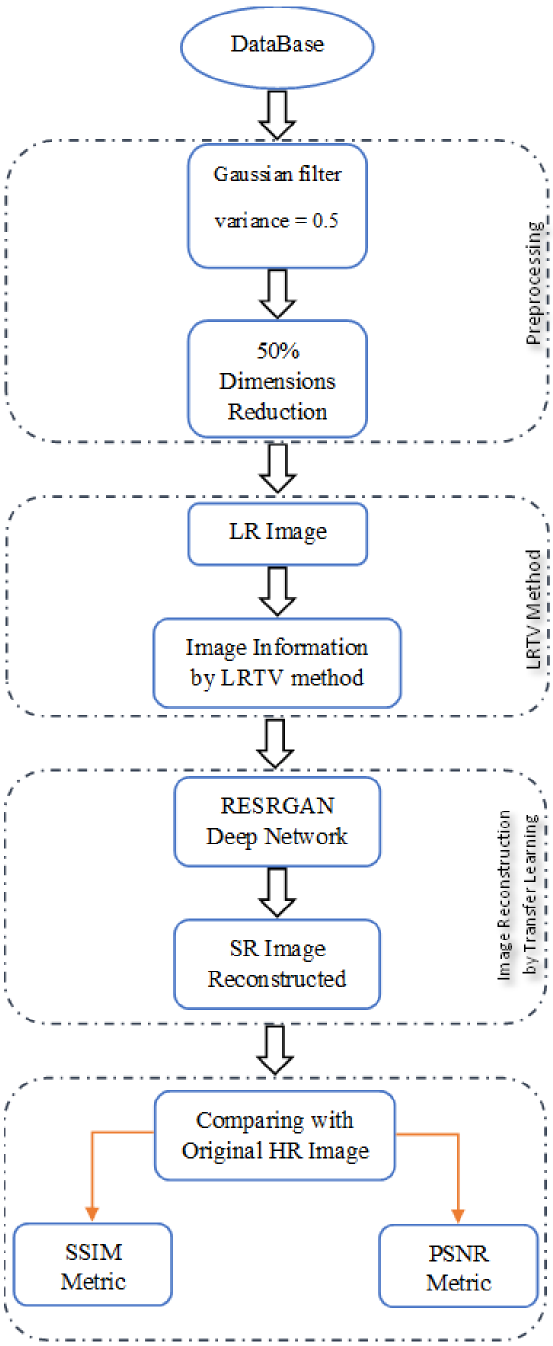

Fig. 4 A detailed workflow of the proposed image super-resolution approach, starting with a Database, applying a Gaussian filter (variance = 0.5) and 50% dimension reduction to create LR images. LRTV method enhances image details, followed by RESRGAN Deep Network with transfer learning for SR reconstruction. Quality is assessed by comparing with original HR image using PSNR and SSIM metrics.

The mean squared error (MSE) represented in Eq. (5), where I_{HR} and I_{SR} represent the original HR image (input) and the super-resolution image (output of the method), respectively. Also, mn shows the dimensions of the images in pixels. PSNR is introduced in terms of decibels (dB) and the higher the value of this number, the greater the similarity between two images. It is necessary to mention that the number obtained from the PSNR metric only compares the intensity values of the pixels of two images and its main focus is on the sensitivity of the noise level [21]. Quantitative results for PSNR and SSIM across the three modalities are summarized in Table 1.

Figures 5−6 present a concise review and comparison of the proposed method and the bicubic method, showcasing the obtained results. The reconstructed images using the proposed method demonstrated a notable improvement compared to the bicubic method. Graphs demonstrate this improvement clearly.

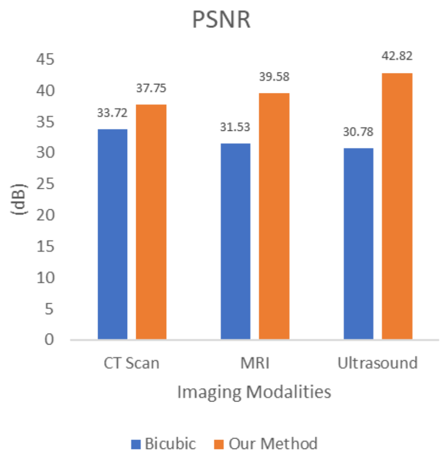

Fig. 5 This chart compares PSNR values (in dB) between bicubic and our method across three imaging types: CT Scan, MRI, and ultrasound. The X-axis represents the imaging types, while the Y-axis shows the PSNR values, indicating image quality with higher values reflecting better quality.

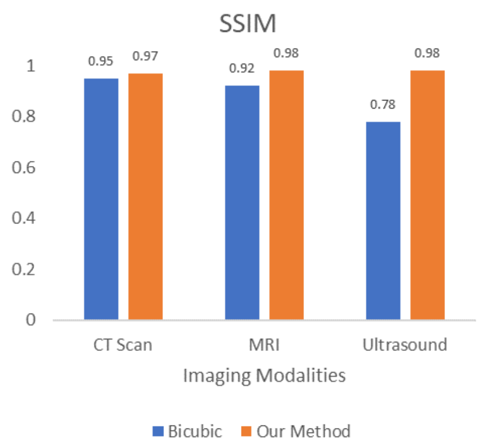

Fig. 6 This chart compares SSIM values between bicubic and our method across three imaging types: CT Scan, MRI, and ultrasound. The X-axis represents the imaging types, while the Y-axis shows the SSIM values, indicating image quality with higher values reflecting better quality.

Table 1 Mean and standard deviation of PSNR and SSIM for quantitative evaluation of the super-resolution approach across different brain image modalities.

Modalities	Metrics	Bicubic method	The proposed method
CT	PSNR	33.77 ± 1.40	37.75 ± 0.90
	SSIM	0.95 ± 0.005	0.97 ± 0.002
MRI	PSNR	31.53 ± 1.62	39.58 ± 2.08
	SSIM	0.92 ± 0.01	0.98 ± 0.005
Ultrasound	PSNR	30.78 ± 1.02	42.82 ± 0.79
	SSIM	0.78 ± 0.03	0.98 ± 0.007

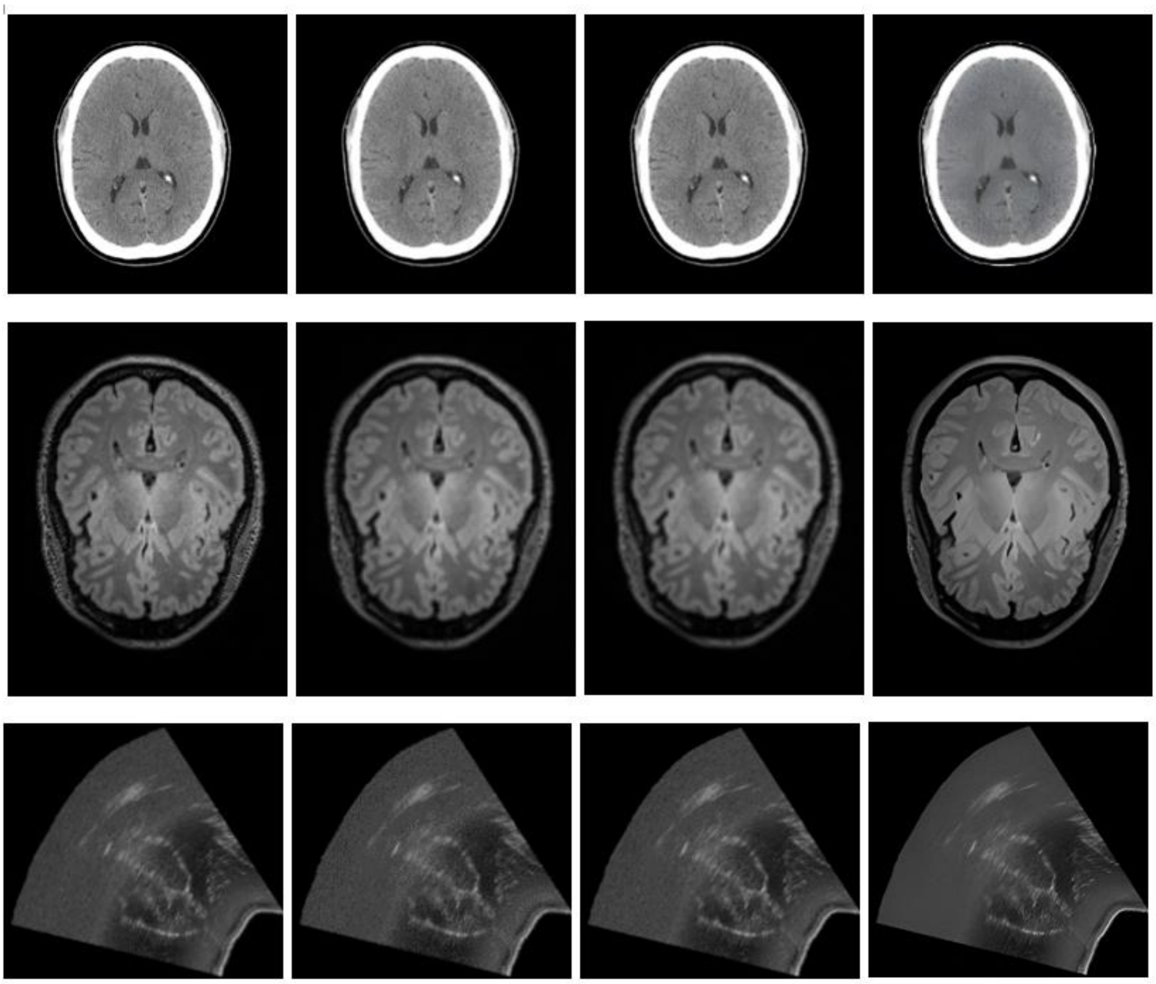

Fig. 7 Comparative analysis of original and enhanced images using various resolution improvement methods. Column (a) original images sourced from databases; Column (b) constructed LR images; Column (c) images reconstructed via the bicubic interpolation method; Column (d) super-resolved images generated by the proposed method.

Figure 7 displays the conversion steps for the original image, including the LR image and the super-resolution image. All three image modalities are depicted in this figure with the first row showing CT scan images, the second row showing MR images, and the third row depicting ultrasound images. The reconstructed images can be visually evaluated to compare the quality of the bicubic method to the proposed method.

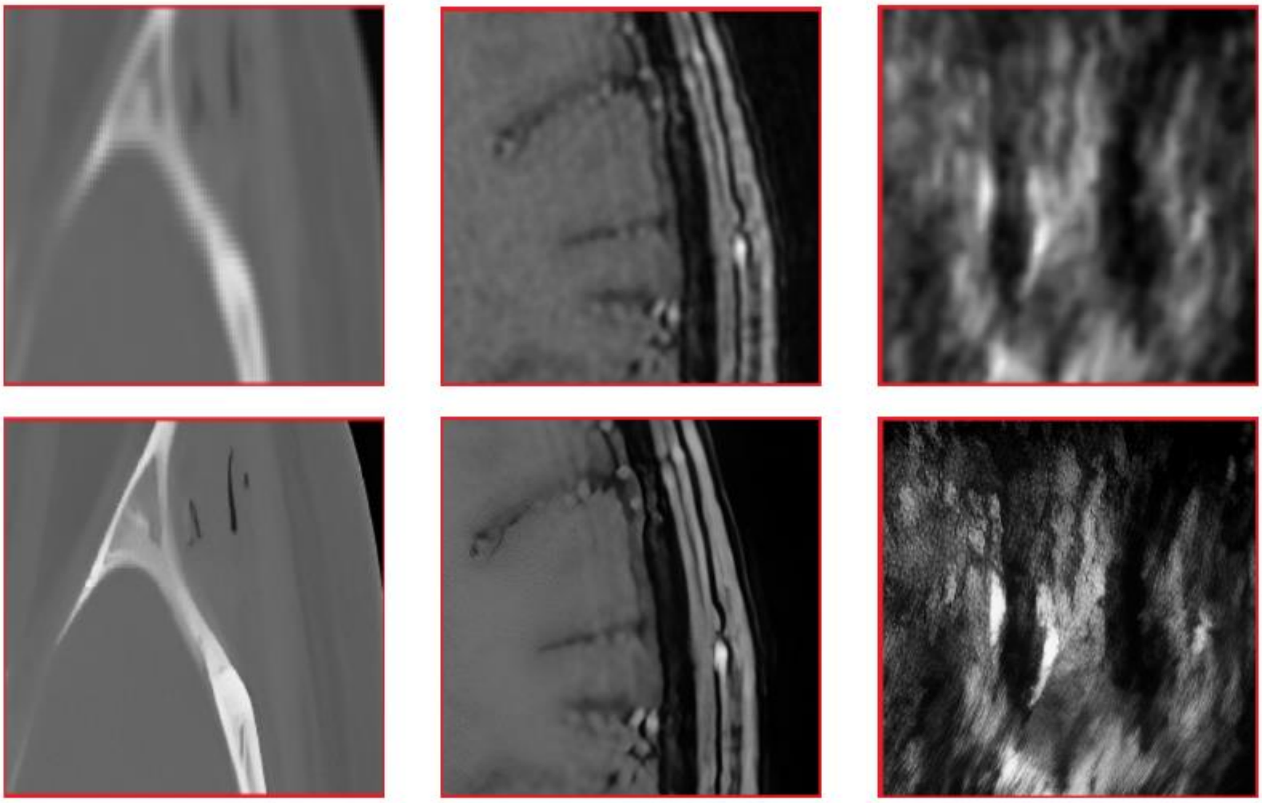

Fig. 8 Visual comparative assessment of original images (top row) versus their corresponding super-resolved images (bottom row), with magnified identical patches provided for detailed inspection, utilized for validating the proposed method. (a) CT scan sourced from the RIRE database [37]; b) MRI and c) ultrasound images obtained from the BITE database [35]. These images, derived from two entirely distinct databases, were employed to ensure robust validation and generalization of the proposed methodology across diverse medical imaging modalities.

One important aim of this study is to establish a strong and complete method for medical imaging systems. For further validation of the proposed method's performance on other systems, we have utilized additional legacy databases. Brain images of tumors for evaluation (BITE) database [35], which includes MRI and ultrasound images of 14 men and women with glioma tumors. A 1.5 Tesla GE Signa EXCITE (General Electric, Milwaukee, WI) was used to acquire the images. the slice thickness is 1 mm and the Images are T1-weighted. Ultrasound images were also acquired with the image acquisition system known by IBIS NeuroNav [36]. The ultrasound machine that used to acquire the images was HDI 5000 (ATL/Philips, Bothell, WA), also the ultrasound probe was a P7-4 MHz phased array transducer. images were displayed with B-mode.

Retrospective image registration evaluation (RIRE) database [37], is used for CT scan images, which is from Siemens DR-H scanner with 28 to 34 slices. The thickness of the voxels in the *x* and *y* directions was equal to 0.65 mm and 4 mm in the *z* direction. These data were solely utilized to evaluate the proposed method's generalization. As access to their corresponding HR images was unavailable, their investigation will be conducted qualitatively and visually.

As shown in Fig. 8, implementing the proposed method on LR images obtained from other databases produces satisfactory results. The images possess superior quality due to the significant details present, such as borders and edges. In addition, the primary information of the images remains intact, and no detrimental alterations are detected.

4 Discussion

An important challenge is to increase the resolution of digital images for higher level processes and stages [38]. After conducting extensive research on super-resolution using deep networks, we decided to specifically investigate the results on medical images. To determine the accuracy and generality of the methods used, three medical images of different modalities were used in this study. In this work, single image super-resolution methods were used to obtain brain images using MR, CT scan, and ultrasound modalities. Due to the absence of two predetermined image qualities, the initial images underwent Gaussian smoothing at a rate of 0.5. Subsequently, the image dimensions were reduced by a factor of 0.5 to create a low-resolution image, which was subsequently used as an input for the neural network to reconstruct the image at high resolution. Combining RESRGAN networks with a method that involves both neighborhood pixels and general image information has led to a novel approach for reconstructing images with higher resolution. Our results demonstrate improvement over previous works, with the PSNR and SSIM validation metrics averaging 40.05 and 98.05, respectively, across all three groups of medical images. These values indicate an improvement of 8.03 dB and 9.49 when compared to the bicubic method for the same metrics. The ultrasound image modality exhibited the highest rate of increase, particularly in the PSNR metric. Based on initial observations, it can be concluded that the method used for this modality outperformed the other two as evidenced by the significantly superior SSIM criterion compared to the other modalities. The PSNR metric measures results in terms of signal-to-noise ratio. In future studies, additional medical image modalities and data can be utilized to evaluate networks with different data sets. Other methods for measuring similarity are necessary as PSNR and similar methods cannot be significantly relied upon. Thus, there is a need for more valid standards to evaluate super-resolution techniques.

5 Conclusion

Enhancing the resolution of medical images is of critical importance, as it directly impacts diagnostic accuracy and clinical decision-making, while also addressing the limitations and high costs of modern imaging systems. In this study, we proposed a hybrid super-resolution framework that combines transfer learning, a RESRGAN, and LRTV regularization. By integrating deep learning with classical approaches, the proposed method achieved superior performance in both quantitative metrics and visual quality. Experimental results confirmed that our framework significantly outperformed conventional bicubic interpolation. Specifically, the proposed method achieved an average PSNR of 40.05 ± 1.25 and SSIM of 0.97 ± 0.004, compared to bicubic interpolation, which yielded 32.02 ± 1.34 and 0.88 ± 0.015, respectively. These improvements demonstrate the method's ability to preserve fine anatomical details and reduce artifacts, leading to clearer and more reliable reconstructions for medical interpretation.

In conclusion, the proposed hybrid framework represents a promising tool for medical image super-resolution. Future research will focus on validating the model on larger and more diverse datasets, exploring additional imaging modalities such as histopathology, and developing more reliable evaluation protocols, such as the feature-based similarity index (FSIM) and the universal image quality index (UIQ), to establish more comprehensive benchmarks. Such efforts will contribute to advancing the field by providing standardized and clinically relevant assessments of super-resolution techniques.

Acknowledgments

The authors acknowledge the assistance of large language models such as ChatGPT (GPT-4o) and Grok (Grok 3), which were employed exclusively for language refinement and improvement of textual coherence in the Introduction and Conclusion Sections. These tools were used solely for literary editing and not for generating scientific content.

Conflicts of Interest

The authors declare that they have no conflicts of interest or competing financial interests related to this work.

References

1. S. Umirzakova, S. Ahmad, L. U. Khan, and T. Whangbo, "Medical image super-resolution for smart healthcare applications: A comprehensive survey," Information Fusion 103, 102075 (2024).
2. W. Lu, Z. Song, and J. Chu, "A novel 3D medical image super-resolution method based on densely connected network," Biomedical Signal Processing and Control 62, 102120 (2020).
3. Z. Chen, X. Guo, P. Y. Woo, and Y. Yuan, "Super-resolution enhanced medical image diagnosis with sample affinity interaction," IEEE Transactions on Medical Imaging 40(5), 1377−1389 (2021).
4. J. Jiang, C. Wang, X. Liu, and J. Ma, "Deep learning-based face super-resolution: A survey," ACM Computing Surveys (CSUR) 55(1), 13 (2021).
5. F. Chen, P. W. Tillberg, and E. S. Boyden, "Expansion microscopy," Science 347(6221), 543−548 (2015).
6. M. H. Kamangar, A. H. Jalalzadeh, "Deep Point Correspondence Estimation and SyN-Based Refinement for Multimodal Brain Image Registration," Contributions of Science and Technology for Engineering 2(3), 18−25 (2025).
7. M. Hashemi Kamangar, M. Rajabzadeh, and A. Jalalzadeh, "Detection of Multiple Sclerosis Lesions in MR Images Based on Convolutional Neural Networks," Future Research on AI and IoT 1(1), 10−17 (2025).
8. K. Yamashita, K. Markov, "Medical image enhancement using super resolution methods," Computational Science – ICCS 2020. Lecture Notes in Computer Science 12141, Springer, Cham, 496−508 (2020).
9. M. Yu, Z. Xu, and T. Lukasiewicz, "A general survey on medical image super-resolution via deep learning," Computers in Biology and Medicine 193, 110345 (2025).
10. M. Jahnavi, D. R. Rao, and A. Sujatha, "A Comparative Study Of Super-Resolution Interpolation Techniques: Insights For Selecting The Most Appropriate Method," Procedia Computer Science 233, 504−517 (2024).

11. Y. Li, B. Sixou, and F. Peyrin, "A review of the deep learning methods for medical images super resolution problems," IRBM 42(2), 120−133 (2021).
12. W. Ahmad, H. Ali, Z. Shah, and S. Azmat, "A new generative adversarial network for medical images super resolution," Scientific Reports 12, 9533 (2022).
13. R. Gupta, A. Sharma, and A. Kumar, "Super-resolution using gans for medical imaging," Procedia Computer Science 173, 28−35 (2020).
14. D. Mahapatra, B. Bozorgtabar, and R. Garnavi, "Image super-resolution using progressive generative adversarial networks for medical image analysis," Computerized Medical Imaging and Graphics 71, 30−39 (2019).
15. X. Li, Y. Wu, W. Zhang, R. Wang, and F. Hou, "Deep learning methods in real-time image super-resolution: a survey," Journal of Real-Time Image Processing 17, 1885−1909 (2020).
16. I. Goodfellow, J. Pouget-Abadie, M. Mirza, B. Xu, D. Warde-Farley, S. Ozair, A. Courville, and Y. Bengio, "Generative adversarial nets," Advances in Neural Information Processing Systems 27, (2014).
17. S. Zhou, L. Yu, and M. Jin, "Texture transformer super-resolution for low-dose computed tomography," Biomedical Physics & Engineering Express 8(6), 065024 (2022).
18. J. H. Ketola, H. Heino, M. A. Juntunen, M. T. Nieminen, S. Siltanen, and S. I. Inkinen, "Generative adversarial networks improve interior computed tomography angiography reconstruction," Biomedical Physics & Engineering Express 7(6), 065041 (2021).
19. X. Wang, L. Xie, C. Dong, and Y. Shan, "Real-esrgan: Training real-world blind super-resolution with pure synthetic data," in Proceedings of the IEEE/CVF International Conference on Computer Vision, 1905−1914 (2021).
20. F. Shi, J. Cheng, L. Wang, P.-T. Yap, and D. Shen, "LRTV: MR image super-resolution with low-rank and total variation regularizations," IEEE Transactions on Medical Imaging 34(12), 2459−2466 (2015).
21. M. Akbari, A. H. Foruzan, and Y.-W. Chen, "A Multi-Cluster Random Forests-Based Approach to Super-Resolution of Abdominal CT Images Using Deep Neural Networks," in 2020 28th Iranian Conference on Electrical Engineering (ICEE), IEEE (2020).
22. F. Deeba, S. Kun, F. A. Dharejo, and Y. Zhou, "Wavelet-based enhanced medical image super resolution," IEEE Access 8, 37035−37044 (2020).
23. W. Shi, J. Caballero, F. Huszar, J. Totz, A. P. Aitken, R. Bishop, D. Rueckert, and Z. Wang, "Real-time single image and video super-resolution using an efficient sub-pixel convolutional neural network," in Proceedings of the IEEE Conference on Computer Vision and Pattern Recognition, 1874−1883 (2016).
24. Y. Gu, Z. Zeng, H. Chen, J. Wei, Y. Zhang, B. Chen, Y. Li, Y. Qin, Q. Xie, Z. Jiang, and Y. Lu, "MedSRGAN: medical images super-resolution using generative adversarial networks," Multimedia Tools and Applications 79, 21815−21840 (2020).
25. L. Chen, X. Yang, G. Jeon, M. Anisetti, and K. Liu, "A trusted medical image super-resolution method based on feedback adaptive weighted dense network," Artificial Intelligence in Medicine 106, 101857 (2020).
26. J. Salvador, E. Perez-Pellitero, "Naive bayes super-resolution forest," in Proceedings of the IEEE International Conference on Computer Vision, 325−333 (2015).
27. Y. Xiao, M. Fortin, G. Unsgård, H. Rivaz, and I. Reinertsen, "REtroSpective Evaluation of Cerebral Tumors (RESECT): A clinical database of pre-operative MRI and intra-operative ultrasound in low-grade glioma surgeries," Medical Physics 44(7), 3875−3882 (2017).
28. Patient Contributed Image Repository (PCIR), "PCIR Official Website," (accessed 25 November 2024) [https://www.pcir.org/].
29. J. L. Lancaster, D. R. McKay, M. D. Cykowski, M. J. Martinez, X. Tan, S. Valaparla, Y. Zhang, and P. T. Fox, "Automated analysis of fundamental features of brain structures," Neuroinformatics 9, 371−380 (2011).
30. MathWorks, "MATLAB R2022b". (accessed 25 November 2024) [https://www.mathworks.com/help/images/ref/volumeviewer-app.html]
31. D. Qiu, L. Zheng, J. Zhu, and D. Huang, "Multiple improved residual networks for medical image super-resolution," Future Generation Computer Systems 116, 200−208 (2021).
32. M. Puttagunta, R. Subban, and N. K. Babu C, "SwinIR transformer applied for medical image super-resolution," Procedia Computer Science 204, 907−913 (2022).
33. W. Zhou, A. C. Bovik, H. R. Sheikh, and E. P. Simoncelli, "Image quality assessment: from error visibility to structural similarity," IEEE Transactions on Image Processing 13(4), 600−612 (2004).
34. O. S. Faragallah, H. El-Hoseny, W. El-Shafai, W. A. El-Rahman, H. S. El-Sayed, E.-S. M. El-Rabaie, F. E. A. El-Samie, and G. G. N. Geweid, "A Comprehensive Survey Analysis for Present Solutions of Medical Image Fusion and Future Directions," IEEE Access 9, 11358−11371 (2021).
35. L. Mercier, R. F. Del Maestro, K. Petrecca, D. Araujo, C. Haegelen, and D. L. Collins, "Online database of clinical MR and ultrasound images of brain tumors," Medical Physics 39(6Part1), 3253−3261 (2012).
36. L. Mercier, R. F. Del Maestro, K. Petrecca, A. Kochanowska, S. Drouin, C. X. B. Yan, A. L. Janke, S. J.-S. Chen, and D. L. Collins, "New prototype neuronavigation system based on preoperative imaging and intraoperative freehand ultrasound: system description and validation," International Journal of Computer Assisted Radiology and Surgery 6(4), 507−522 (2011).

37. J. West et al., "Comparison and evaluation of retrospective intermodality brain image registration techniques," Journal of Computer Assisted Tomography 21(4), 554−568 (1997).
38. M.-I. Georgescu, R. T. Ionescu, A.-I. Miron, O. Savencu, N.-C. Ristea, N. Verga, and F. S. Khan, "Multimodal multi-head convolutional attention with various kernel sizes for medical image super-resolution," in Proceedings of the IEEE/CVF Winter Conference on Applications of Computer Vision (WACV), 2195−2205 (2023).